FUSION OF SYNTHETIC APERTURE RADAR AND OPTICAL SATELLITE DATA FOR UNDERWATER TOPOGRAPHY ESTIMATION IN COASTAL AREAS

Andrey L. Pleskachevsky(1), **Susanne Lehner**(1)

(1) *German Aerospace Centre (DLR), Remote Sensing Technology Institute, 82234 Weßling, Münchener Str. 20, Germany), Email:Andrey.Pleskachvsky@dlr.de*

ABSTRACT

A method to obtain underwater topography for coastal areas using state-of-the-art remote sensing data and techniques worldwide is presented. The data from the new Synthetic Aperture Radar (SAR) satellite TerraSAR-X (TS-X) with high resolution up to 1m are used to render the ocean waves. As bathymetry is reflected by long swell wave refraction governed by underwater structures in shallow areas, the bathymetry can be derived using the dispersion relation from observed swell properties. To complete the bathymetric maps, optical satellite data of the QuickBird satellite are fused to map extreme shallow waters, e.g., in coast near areas. The streak structures produced by SAR imaging of the wave breaking at the shore are investigated. This allows estimating the amplitude of the breaking wave before keeping.

1. INTRODUCTION

In this paper the different remote sensing data are combined to collect the underwater topography in costal areas worldwide. In spite of the fact that the worldwide bathymetry should already be known, and there are no "blank spots" on global maps, at least for 1 nautical miles resolution data sets (e.g. global topography by NOAA, ETOPO 1-Minute Global Relief, NOAA) the local depth variation e.g. sand bank, bars and reefs on the one hand and temporal morphodynamical development of seabed structures on the other hand can be significant in littoral zones. E.g. in the German Bight (North Sea), the soft seabed topography can changes relatively fast due to storms so that the official charts can be quite out of date.

Generally, the remote sensing techniques to obtain high resolution bathymetry can be divided in to two groups, based on the physical background of algorithms:

(1) depth estimation from remote sensing data, based on sunlight reflection analysis and governed by chemical and physical characteristics of sea water, e.g. the bottom reflection. This kind of investigations is covered by optical methods: processing optical satellite data allow physical approximations of the water depths by correcting sunglint, atmospheric effects and the influence of the water column in the earth observation data **[1]**.

(2) depth estimation based on observation of hydrodynamic processes, which are influenced by topography in a different way and thus reflect the underwater structures. This group of technique can be performed using SAR (e.g. **[2]**), RAR (marine Real Aperture Radar, e.g. WAMOS, **[3]**) and optical data **[4]**.

In the paper, both of the techniques mentioned are applied. The investigations are carried out near Rottenest Island, Australia, where SAR, optical and echo-sounding *in-situ* measurement data are available. The area investigated is indicated by a sliced shore line, complicated underwater topography which includes numerous underwater reefs and is a real challenge for an algorithms "robustness test".

Both techniques: depth estimation from optical information for extra-shallow water and non-direct technique using SAR data have been effectively tested in different areas **[2]**, but a combination of their results into an aggregate product is the new topic presented in the paper.

Depth data sets obtained from optical images (QuickBird) and from SAR (TerraSAR-X) are combined in order to cover different depth domains. The SAR-based and optical approaches to estimate bathymetry make use of different physical backgrounds, have different mathematical implementations and acquisition conditions. The SAR-based methodology uses long wave refraction; it can not be applied during a calm weather conditions prefer for optical methods. The waves produce seabed erosion and influence light attenuation in water column by suspended matter. Otherwise, results from SAR and optical data complement each other: The optical methods provide reliable depths in domain up to 20m (the results are depending on the Specific Inherent Optical Properties (SIOP) of the analysed water body). The depths estimation from SAR cover domain about 70m-10m, obtained from wave behaviour, and is dependent on wave properties and acquisition quality. The depth between 10m and 25m is the potential synergy domain there data from both sources can be compared and integrated.

In this paper the underwater topography for the Rottenest Island, Australia is investigated. The selection of this domain has several backgrounds:

Proc. of 'SEASAR 2012', Tromsø, Norway
18-22 June 2012 (ESA SP-709, March 2013)

(1) depth data from sonar measurements of fine spatial resolution are available,
(2) the water attenuation (the island is a fossilized coral reef) allows depth estimation using optical data in the coastal zone.
(3) the storms in the south-west of Australia create well developed and reliably forecasted long swell directed to the study area.

Rottenest Island is situated about 50km off the coast of Western Australia, (115°30'E, 32°00'S) near of the city of Perth. The Island is about 10.5km long and 4.5km wide and located on the relatively flat continental shelf off the Perth coastline. The Island presents the seaward end of the shallow Murray Reef System; thus the western end of Rottenest Island can be considered a headland. The notch of the angular-shaped shelf edge, which is the beginning of the Perth submarine canyon, is located off the island's western end.

2. DATA AND METHOD

The German X-band SAR satellite TS-X was launched in June 2007. Since January 2008, data and products are available for researchers and commercial customers. TS-X operates from a 514km height sun-synchronous orbit. The TS-X ground speed is 7km·s^{-1} (15orbits/day). It operates with wavelength 31mm and frequency 9.6GHz. The repeat-cycle is 11 days, but the same region can be imaged with different incidence angles after three days dependent on latitude. There are four different imaging modes with different spatial resolution, technical parameters of the different modes are provided. The resolution of TS-X images have been visible improved in comparison to earlier SAR missions (about 2m for Spotlight mode against 25m for ENVISAT ASAR). Typical incidence angles for TS-X range between 20° and 60°.

Compared to earlier SAR missions like ENVISAT ASAR, TS-X offers besides higher resolution a number of further advantages: e.g. the Doppler-shift of a scatterer, moving with radial velocity u_r toward the sensor (radial velocity) at distance R_o (slant range) is reduced. For instance, for the same incidence angle 22° and u_r=1m·s^{-1} the target's displacement in azimuth direction $D_x = (u_r / V_{sar}) \cdot R_o$ is reduced by a factor about two and results in ~73m for TS-X (~115m for ENVISAT) due to different platform velocity V_{sar} (7,55km·s^{-1} for ENVISAT) and slant range R_o (ENVISAT altitude is 800km) **[5]**.

The analysis of TS-X images can be used for the following oceanographic applications: ship-, ice-, oil- and underwater shallow area (bank and bars) detection, obtaining wind, costal line and underwater topography fields **[6]**. In the following the TS-X Spotlight model images with coverage of 10km by 10km and resolution of 1m were used. For this mode, the SAR azimuth resolution is improved by pointing the antenna towards the specific target area (spot) during overflight. This increases the time-bandwidth product and improves the resolution. Fig.2. shows the effect of the achieved higher resolution comparing images of ENVISAT with a pixel size of 12m to TS-X images. The ENVISAT scene was acquired on December 21, 2008 over Rottenest Island; the sub-scenes for location in front of the east-coast of the Island are shown for TS-X Spotlight, Stripmap and ENVISAT. Although the waves are detectable in ASAR images, extraction of wavelength <200m and obtaining refraction of quality necessary for underwater topography estimation is not possible (zoomed cuts from the images see Fig.1, complete scene see Fig.2).

For the TS-X properties, the imaging of swell wave with length L=100m and amplitude of a=1.5m, period of T=10s, (maximal orbital velocity at the crest u_{orb}=0.98m·s^{-1}) traveling in azimuth and in opposite to satellite flight direction produces the velocity bunching of 75m for incidence angle θ=22°. Although the imaging mechanism is non-linear according to conventional theories, the replacing of the facets remains inside of one wave length for TS-X characteristics (ground speed and slant range). The wave is imaged "turned" in location of **[7]**. The comparison over 100 TS-X scenes acquired over collocated buoys shows the correlation of 0.95 for peak direction derived from images and in-situ measurements (R^2=0.89, SI=0.19).

The method is based on observation of consecutive waves along their propagation from a start point up to the coast. The wave-rays technique is already well

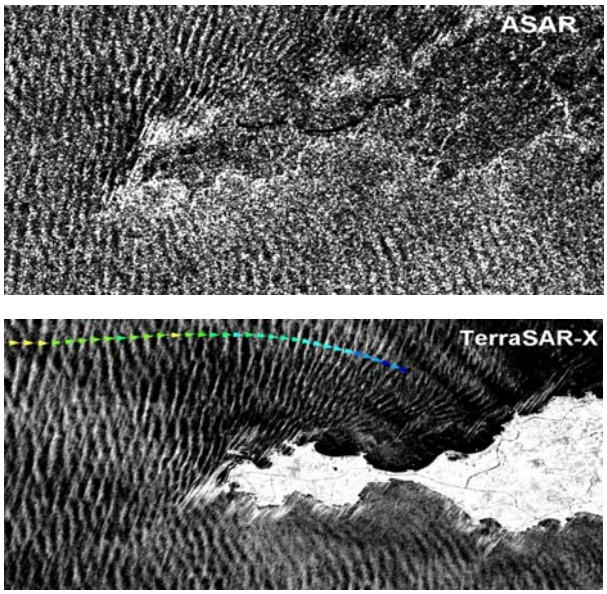

Figure 1. Rottenest-Island, ASAR (resolution ~25m, image pixel size 12m) and TerrsSAR-X Spotlight (resolution ~2m, image pixel size 0.75m) (zoom): Although the waves are detectable in ASAR images, extraction refraction and underwater topography is not possible.

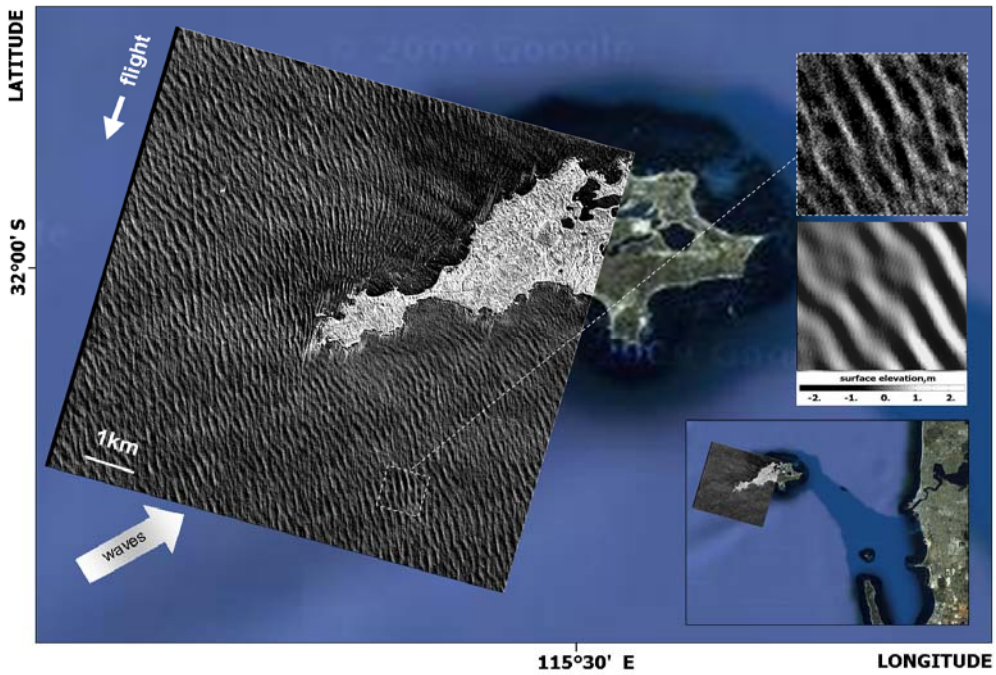

Figure 2. TerraSAR-X Spotlight 10km by 10km coverage acquired on October 20, 2009 over Rottenest Island Australia (background image © Google Map). A sub-scene (top right) shows details of the wave structures and random surface elevation obtained from wave spectra simulated by a numerical model.

known and widely used as an application for the wave model results. The wave rays can be obtained also from wavelength and wave direction observed on SAR images. By computing the FFT-analysis for the selected sub-image a two dimensional image spectrum in wave number space is retrieved. The peak in the 2-D spectrum marks mean wavelength and mean wave direction of all waves visible in the sub-image. Values for wavelength and angle of wave propagation can be estimated as follows:

$$L_P = \frac{2\pi}{\sqrt{k_{Px}^2 + k_{Py}^2}}, \quad \theta_P = \arctan\left(\frac{k_{Py}}{k_{Px}}\right) \qquad \textbf{(1)}$$

where L_P is the peak wavelength, θ_P is the peak wave direction with respect to the image (azimuth direction), k_{Px} and k_{Py} are the image spectra peak coordinates in wave number domain with axes x= satellite flight direction (azimuth) and y=range. The retrieved wave directions have an ambiguity of 180° due to the static nature of a SAR image. This ambiguity can be resolved using SAR cross spectrum or first guess information from other sources. In coastal areas where wave shoaling and refraction appears, the propagating direction towards the coast is visible on the image.

Starting in the open sea the box for the FFT is moved in wave direction by one wavelength (or with a constant specified shift) and a new FFT is computed. The procedure is repeated until the corner points of the FFT-Box reaches the shoreline. This way waves can be tracked from open sea to the shoreline and changes of wavelength and direction can be measured **[2], [7]**.

To retrieve water depth, the linear dispersion relation for ocean gravity waves was applied. The solution of the dispersion relation with respect to water depth d:

$$d(L_P, \omega_P) = \frac{L_P}{2\pi}\,\mathrm{atanh}\left(\frac{\omega_P^2 L_P}{2\pi g}\right) \qquad \textbf{(2)}$$

where ω_P is the angular wave peak frequency ($\omega_P = 2\pi/T_P$, T_P is the peak period). The method was approved for different areas and sea states **[2],[7]** i.e. for the Duck Research Pier (North-Caroline, USA), Port Phillip (Melbourne, Australia), and around Helgoland Island (German Bight, North Sea).

3. RESULTS SAR

The Spotlight TS-X SAR image acquired over Rottenest Island on October 20, 2009 is shown in Fig.2. The long-swell waves induced in Ocean due to storm (storm peak about 1500km south-west from the area three days before) and propagating towards the island are visible in the TS-X image and the refraction is well pronounced. The scene was specially ordered to acquire the long swell waves for bathymetry estimation. The wave forecast model WAVEWATCH-III (NOAA) was used to determine the appropriate acquisition time. The forecasting information was applied one week before TS-X image acquisition. For the practical use, obtaining topography is divided into five workflow steps:

(1) scene first-check: simulation of some wave tracks (e.g. ten reference tracks). Reference tracks overlap the study domain in different

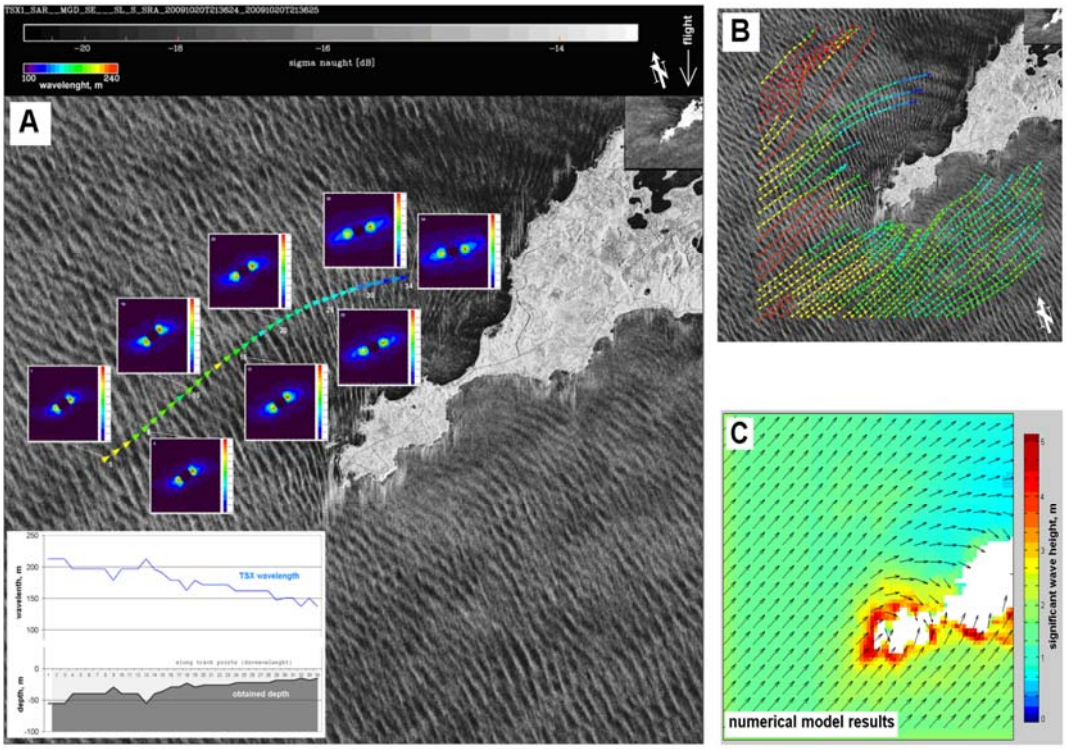

Figure 3. TerraSAR-X Spotlight acquired over Rottenest Island (Fig.2). NRCS and one wave track with exampling image spectra are shown (A). Sub-scene shows the wavelength along the track and obtained underwater topography for its trajectory. In the top-right corner the quicklook of the scene is shown. 40 wave rays overlap the area are shown (B). Numerical simulation (C) presents significant wave height and refraction (direction shown by arrows, model inputs are wind field and boundary estimated from TS-X data, horizontal resolution is 150m, bathymetry is based on NOAA dataset). The shoaling areas are presented by strong increasing of wave height; since the bank in the north of the Island is not present in the coarse NOAA bathymetry, no refraction occurs at this location in model simulation.

areas. First-checking is applied to evaluate the validity of the scene, to obtain the threshold for filtering of wavelengths and directions. Further, the peak period is estimated: this determination obtaining wavelength map using wave ray technique: a dense coverage of the area with waves tracks. For uniform mesh (150m resolution) 400 wave rays were necessary for sufficient dense area coverage.

(2) obtaining wavelength using raster method: in the areas where coverage of wave tracks is not dense enough, a raster approach is used: the FFT-boxes are moved not in the wave direction, but at a certain distance *dx* and *dy*.

(3) obtaining resulting wavelength field: after filtering, wavelength is interpolated, extrapolated and smoothed on a uniform grid (a reasonable resolution for topography is the averaged wavelength, for Rottenest Island the raster $dx=dy$ =150m was applied).

(4) estimation of corresponding depths: using the dispersion relation the depth field is derived.

The peak period, needed in eq.2 is obtained using combination of first guess and analysis of the tracks (T_p=13.25sec). The longest observed wave in the image is L_{max}=245m. The threshold for minimal peak period for this wavelength, obtained from deep water relation $T_p^{min}=(2\pi L_{max}/g)^{0.5}$=12.25s (by solutions of dispersion relation for periods smaller than 12.5s, belongs wave of length of 245m to deep water domain, where it cannot be influenced by bottom. Then again the wave length changes in the SAR image that evidences the bottom influence, thus $T_p>T_p^{min}$).

Fig.4 shows the scene processing results: derived wave field (Fig.4a), derived underwater depth field (rectangular mesh of 150m horizontal resolution, shown 3-D, Fig.4b). Fig.4c presents the scheme for comparison of retrieved data with sonar measurements: The TS-X scene is underlying, a white line marks the area for which a comparison is done. The sonar measurement data from different echo-sounding campaigns (measurement errors unknown) are also integrated and interpolated on rectangular uniform grid $dx=dy$=150m, then about 50% of the compared area has an error range of about +/-10% (shown in white colour). There are also more variations (one is located in the north of the Island: the swell waves are slowed down and dissipated over a reef and do not build up anymore in a “bag” between two reef-banks.

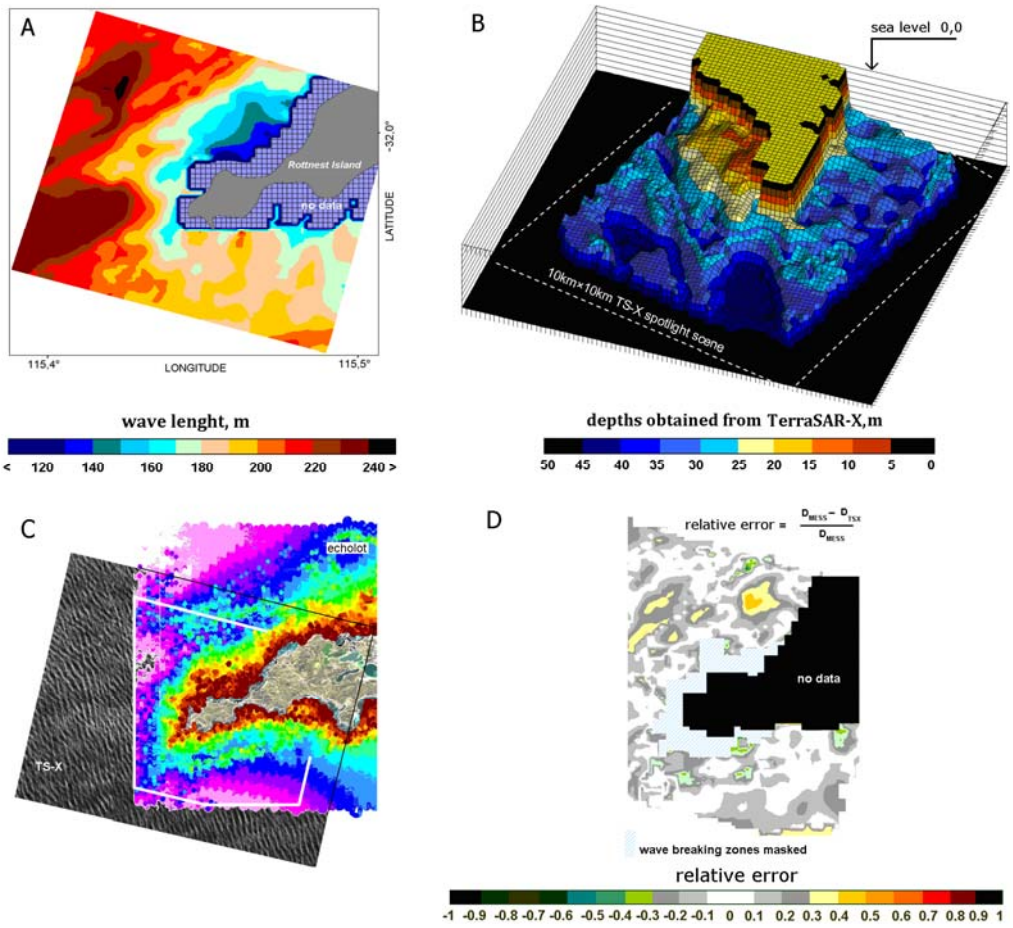

Figure 4. Wavelength field (uniform raster 150m resolution) obtained from TS-X scene (A), 3-D depth field derived (B), schema for comparison of a sonar measurement to TS-X derived depths (white line marks the comparison area) (C) and relative error for white marked area (wave breaking zones are masked additionally) (D)

The wave breakings zones, in front of the coast destroy the processing of sub-images and do not allow obtain the wave length accurately. They are masked and taken out from depth estimation processing.

4. SYNERGY AND DATA FUSION

The depths estimation from SAR covers the areas between about 100m and 10m water depths, depending on sea state and acquisition quality. The optical methods require other physical conditions the SAR-based methods and provide the depths shallower than 20m. The depths between 10m and 25m are a potential synergy domain where data from both sources can be incorporated. In order to obtain incorporated depth field the study area is divided into three sub-areas:

1) SAR data domain: area deeper than about 20m. In this area, only the SAR data can be used, as for optical methods the seabed is too deep.
2) synergy area with depths between about 20m and 10m. In this region, the estimated depths from SAR and optic overlap each over.
3) optical data domain: coastal shallow waters shallower than 10m: in this area only optical data can be applied, the swell waves becomes nonlinear and break.

In order to obtain the depth field for a uniform raster (*case A)* the optical data must be averaged for the coarser resolution and incorporated with SAR obtained data. Different methods for data combination can be used, e.g. method of optimum interpolation. Fig.5 (left) presents the resulting depth filed on a uniform rectangular raster of 150m horizontal resolution. The depths between 60m and 20m is based on SAR data only, the depths lower then 20m are combination of SAR and optical information. The presented underwater depth field includes bathymetry up to mean sea level and can be combined with above-water topography. Thus, the data from TanDEM-X mission can be incorporated in order to retrieve the complete digital elevation model. The data are combined also without averaging and keeping original information. The Fig.5 (right) shows the data aligned on an irregular mesh (150m for SAR-domain and 2.4m for optic domain).

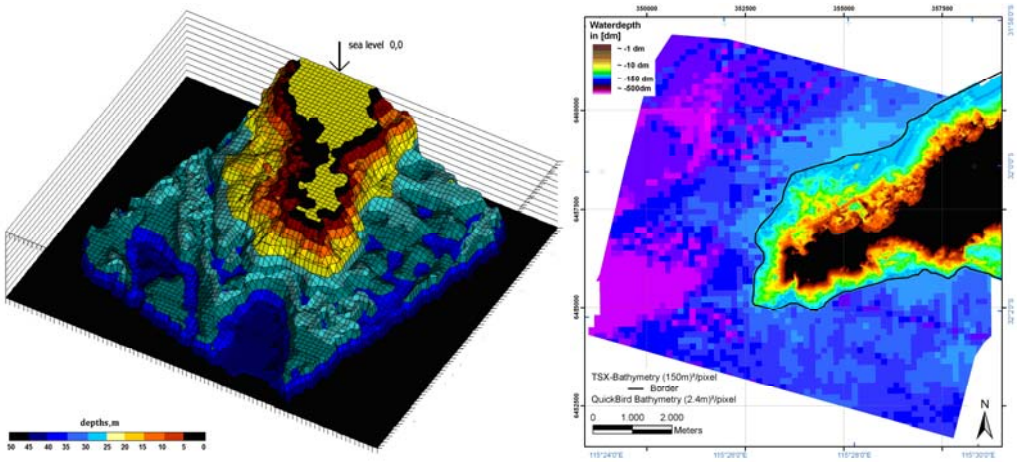

Figure 5. Depth field obtained from TS-X SAR and optical QuickBird data after fusion and synergy were applied on uniform raster with horizontal resolution of 150m by 150m. The resulting bathymetry field covers the area about 8km by 8km (left). Depth field obtained from TS-X and optical data applied on non-uniform raster (150m for SAR domain and 2.4m for optical domain, right).

The borderline between the two data sets was defined by visual means at a depth of 18m to 20m, where the results of the 'optical' depth analysis start to decrease in reliability.

5. WAVE BREAKING

As a wave is shoaling, wave height increases, which leads to an increae of the orbital velocity of water particles within the wave. The shoaling occurs until wave steepness exceeds a certain threshold where wave breaking takes place (condition: the orbital velocities in the wave exceed the phase speed of the wave). The breaking produces an area with increased turbulence and surface roughness which causes a strong radar echo. Additionally, smearing is caused by Doppler shift due to high radial velocities of the scatterers. The streak structures at such locations are investigated and their length was used to estimate the maximal radial speed of the scatterers and consequently the speed at the crest of the breaking wave and the wave amplitude.

Fig. 6 shows an example for Rottnest Island and a cut of wave height simulated using the numerical spectral wave model and using the shoaling coefficients from wave height at the boundary (no dissipation and breaking). The value at the coast retrieved by the model is 5m, the shoaling coefficient simulation results in about 7m. The estimation from using SAR is about 4m. Fig.7 shows an example for the Somalia coast displayed on Google Earth.

6. RELATION TO SHIP DETECTION

Development of algorithms and methods for remote sensing data processing are carried out along two main lines. On one hand, satellite images taken by space borne sensors are used to explain atmospheric as well as oceanographic geophysical processes and features, e.g. wind field and sea, on the other hand products for NRT services, such as ship detection are provided. Knowledge of basic geophysical processes and its imaging mechanism by remote sensing is necessary for successful processing of images **[8]**. For instance, for ship detection the SAR image background plays a major role. The "white capping" and wave breaking can produce turbulence at the sea surface, which causes a high radar backscatter and could be falsely detected as a ship. However, these can take place for local wind speed higher than about $12 m \cdot s^{-1}$. For lower wind speed the breaking structures observed would show the hindrance like a reef or underwater bank, which forces a wave to overturn. Thus, wind speed estimation is necessary to provide information for filtering and image interpretation. All this information is contained in the images and must be properly extracted, assessed and applied (see Fig.8).

SUMMARY

A practical approach for exploring of bathymetry by synergetic use of multiple remote sensed data sources for coastal areas is presented. The SAR-based method uses refraction of swell waves and covers tdepth domain between 100m and 10m. The optical-based method uses sunlight reflection analysis and covers the depth interval shallower than 20m.

The underwater topography is obtained with accuracy of the order of 15% for depths 60m-20m using SAR-based method. The estimation accuracy is dependent on sea state (swell wave length) and its acquisition quality. The latter is influenced by artefacts, nonlinear SAR-imaging effects and the complexity of the topography itself (e.g. reefs cause wave breaking).

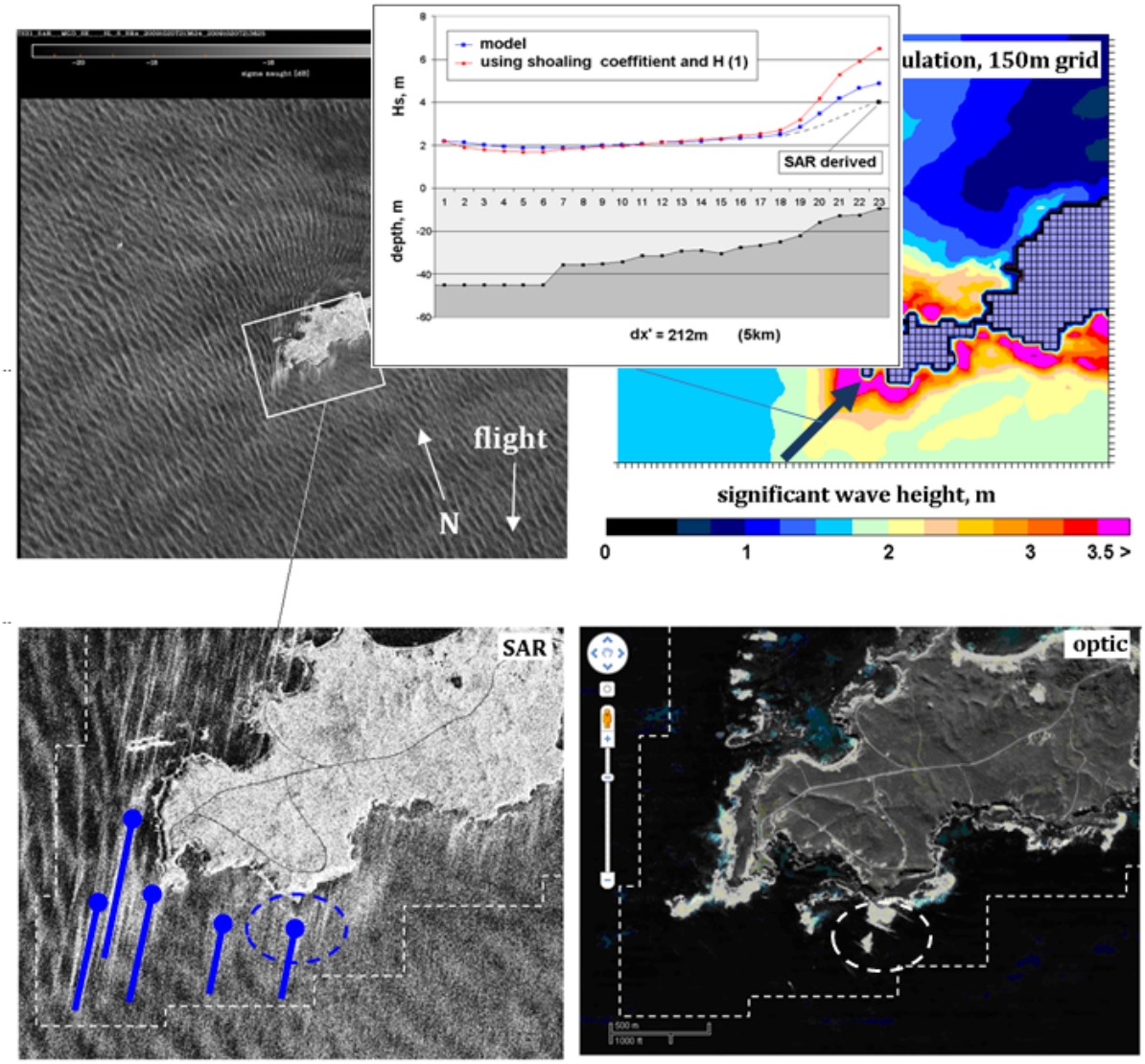

Figure 6. TS-X Spotlight image (top left) and a zoom show swell wave breaking and breaking structures in front of the coast (bottom left). The result of numerical simulation (top right, significant wave height) shows strong shoaling effect by increased wave height over coral reef-belt. An optical image © Google Earth (wave breaking location are visible).

Additionally, the SAR-based methodology allows the detection of shoals (underwater mountains, reefs, deposited sand bars) with depths <30m, even if the quality of sea state is insufficient for obtaining the topography with the mentioned accuracy. The remote sensed information on shoals detected can be integrated into maritime ship safety concepts. Furthermore, this kind of data is considered as valuable in areas like German Bight, where topography changes comparably fast due to soft seabed by storms, so that official charts can be out of date. Synoptic and frequent *in-situ* measurements of the German Bight are complicated and expensive procedure. Therefore, the obtained information can be tactically used for supporting *in-situ* measurements performed with e.g. ship borne sonar by pointing out the shallow locations to be updated.

REFERENCES

[1] T. Heege, J. Fischer, "Mapping of water constituents in Lake Constance using multispectral airborne scanner data and a physically based processing scheme". *J. Remote Sensing*, Vol. 30, No. 1, pp. 77-86., 2004.

[2] S. Brusch, P. Held, S.Lehner, W.Rosenthal, A. Pleskachevsky,"Underwater Bottom-Topography in coastal areas from TerraSAR-X data",*International Journal of Remote Sensing*. Vol. 32, Issue 16, 2011.

[3] K. Hessner, K.Reichert, K. and W. Rosenthal, „Mapping of sea bottom topography in shallow water by using a nautical radar". In 2nd International Symposium on operationalization of remote sensing, 16-20 August 1999, Enschede, The Nederlands. 1999

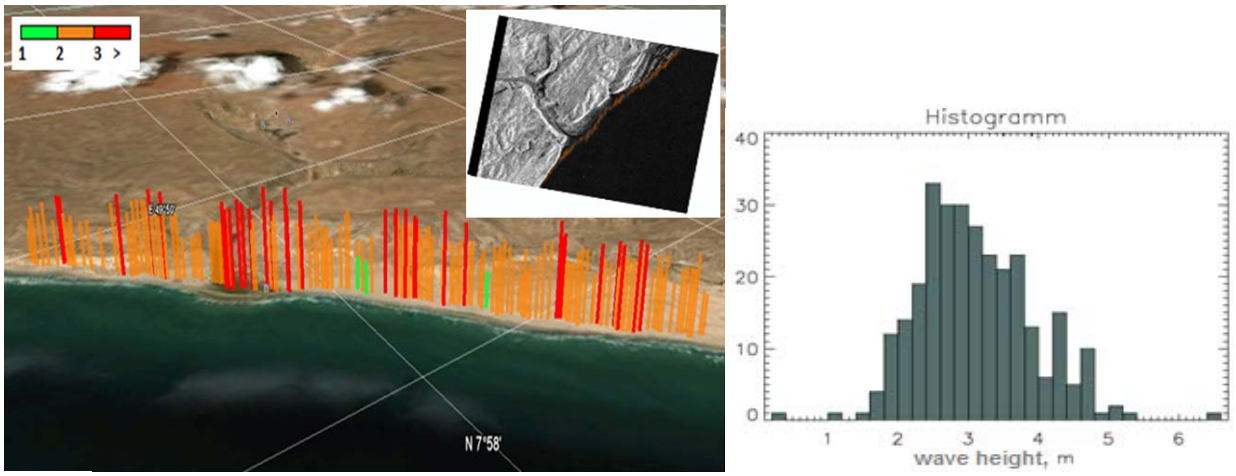

Figure 7. Height of individual breaking waves for Somalia coast from TerraSAR-X Spotlight image displayed on Google Earth

[4] C. Piotrowski, and J.P. Dugan, "Accuracy of bathymetry and current retrievals from airborne optical time-series imaging of shoaling waves". *IEEE Transaction on Geoscience and Remote Sensing,* **40**, pp. 2606-2618. 2002.

[5] D. Lyzenga,.R. A. Shuchman, and J. D. Lyden, "SAR imaging of waves in water and ice: evidence for velocity bunching", J. Geophys. Res., 90, 1031–1036. 1985.

[6] S. Lehner, A.Pleskachevsky, M. Bruck, "High resolution satellite measurements of coastal wind field and sea state", *International Journal of Remote Sensing*, in print.

[7] A. Pleskachevsky, S. Lehner, T. Heege, C. Mott, „Synergy of Optical and Synthetic Aperture Radar Satellite Data for Underwater Topography Estimation the in Costal Areas". *Ocean Dynamics,* 2011.

[8] Lehner, S., Pleskachevsky, A., Brusch, S., Bruck, M., Soccorsi, M., and D. Velotto, "Remote Sensing of African Waters using the High Resolution TerraSAR-X Satellite", (submitted).

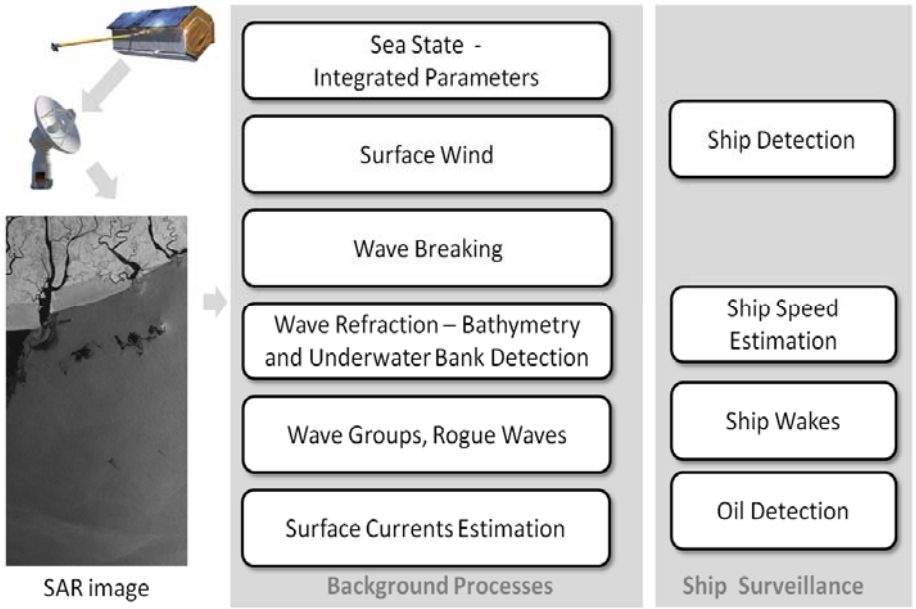

Figure 8. Using remote sensing data for ship surveillance. A wide spectrum of features and processes are involved. The knowledge of the background geophysical processes and their imaging mechanism is important for a robust ship detection services in terms of safety and security.